Accepted Manuscript

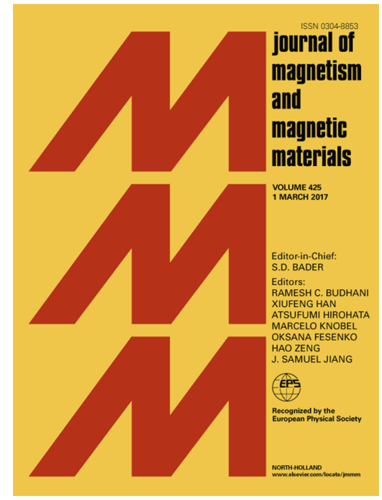

Evidence for reentrant spin glass behavior in transition metal substituted Co-Ga alloys near critical concentration

Sk. Mohammad Yasin, V. Srinivas, S. Kasiviswanathan, Megha Vagadia, A.K. Nigam

PII: S0304-8853(17)32320-X
DOI: https://doi.org/10.1016/j.jmmm.2017.11.061
Reference: MAGMA 63401

To appear in: *Journal of Magnetism and Magnetic Materials*

Received Date: 24 July 2017
Revised Date: 14 November 2017
Accepted Date: 15 November 2017

Evidence for reentrant spin glass behavior in transition metal substituted Co-Ga alloys near critical concentration

Sk Mohammad Yasin, V. Srinivas* and S. Kasiviswanathan

Department of Physics, Indian Institute of Technology Madras, Chennai 600 036, India

Megha Vagadia and A. K. Nigam

Department of Condensed Matter Physics and Materials Science, Tata Institute of Fundamental Research, Mumbai 400 005, India

*Email: veeturi@iitm.ac.in

Abstract

In the present study magnetic and electrical transport properties of transition metal substituted Co-Ga alloys (near critical cobalt concentration) have been investigated. Analysis of temperature and field dependence of dc magnetization and *ac* susceptibility (ACS) data suggests an evidence of reentrant spin glass (RSG)phase in $Co_{55.5}TM_3Ga_{41.5}$ (TM = Co, Cr, Fe, Cu). The magnetic transition temperatures (T_C and T_f) are found to depend on the nature of TM element substitution with the exchange coupling strength Co-Fe>Co-Co>Co-Cu>Co-Cr. From magnetization dynamics precise transition temperatures for the glassy phases are estimated. It is found that characteristic relaxation times are higher than that of spin glasses with minimal spin cluster formation. The RSG behavior has been further supported by the temperature dependence of magnetotransport studies. From the magnetic field and substitution effects it has been established that the magnetic and electrical transport properties are correlated in this system.

1. Introduction

Recent observation of phenomena, such as, unconventional superconductivity, metal-insulator transitions and Quantum Griffiths Phase transition [1-4] in complex band structure alloys has prompted researchers to either re-examine the materials investigated earlier or search for new materials that exhibit complex band structure. For example, both experimental results and theoretical band structure calculations on Fe-based binary, ternary alloys suggested the presence of pseudogap of the order of 0.1 eV near Fermi level, have attracted considerable attention due to their remarkable magnetic and electrical transport properties [5-7]. In particular significant theoretical and experimental efforts have been devoted in understanding the physical properties of transition-metal (TM) aluminides, silicides and gallides with composition close to their magnetic instability [1-9]. They exhibit exotic properties, such as, giant magnetoresistance (GMR), large thermopower and giant Hall effects. Similarly, the electric and magnetic properties of Fe-Al, FeCo-Si, Ni−Al and Co−M (M = Al, Ga) etc intermetallic compounds [7-13] have also been investigated for several years, yet the origin of unusual physical properties observed in these systems eluded the scientific community. For example, whether Fe-Al alloys in the dilute limit lose their moment due to spin fluctuations or hybridization [8]. While finite degree of itinerancy in the ferromagnetic character of Co-doped FeSi alloys has been reported. In such systems where short range ferromagnetic order persists at temperatures above their Curie temperature also exhibit interesting magnetotransport behavior [7]. Similar magnetic and electrical transport behavior has been reported in perfectly ordered equiatomic CoGa compound. Unusual properties like: (i) nonmagnetic down to low temperature despite having 50% magnetic constituent (ii) unlike metallic alloys it exhibits higher resistivity (ρ) values and negative temperature coefficient of resistivity (TCR), despite the presence of metallic elements as constituents (iii) physical properties are highly sensitive to impurities and process conditions, reminiscent of semiconductors (iv) exhibits a range of magnetic phases (antiferro to ferromagnet) with an increase of 10 at% Co with the same crystal structure. Recent studies on Co_xGa_{100-x} (x = 54-61.5) alloys, suggested that at a critical concentration $x_c \approx 57$ a reentrant spin glass (RSG) behavior evolves from cluster spin glass state ($x < x_c$) [14]. The coexistence of non-magnetic and non-metallic behavior in $Co_{50}Ga_{50}$ alloy and subsequent increase in electrical conductivity and magnetic moment on addition of Co appear to satisfy the Stoner criterion and suggest itinerant magnetic character.

Earlier studies showed that the evolution of magnetic moment from non-magnetic $Co_{50}Ga_{50}$ with the increase in Co content and attributed to the antisite disorder [12,15]. However, these studies were unable to probe the roles of Ga and Co independently due to rapid changes in their magnetic character. In order to investigate the effect of site disorder and exchange coupling we have substituted magnetic (Fe, Cr) and nonmagnetic (Cu) elements at Co site and investigated the structural and magnetic properties. Interestingly, the earlier neutron diffraction studies on Ga-poor Co(Ga,TM) alloys revealed that the TM preferentially occupy the Ga sub-lattice and therefore, crystallographically, no distinction appears between these substituted compositions and Co-rich binary series in which excess Co atoms populate Ga sublattice [12]. In the present investigation we have investigated the magnetic and electrical transport properties of $Co_{58.5-x}TM_xGa_{41.5}$ (TM = Cr, Cu, Fe) alloys to unravel the role of magnetic interactions without changing Ga content. The nature of magnetic transitions and the magnetic ground state of the compositions has been studied using static and dynamic magnetic measurements. Further a correlation between magnetic and electrical transport properties has been established through temperature and field dependence electrical resistivity measurements.

2. Experimental details

The alloy ingots with nominal compositions $Co_{55.5}TM_3Ga_{41.5}$, TM = Co, Fe, Cr, Cu were prepared using high purity elemental constituents in an arc-melting furnace under argon atmosphere. Subsequently the ingots were annealed at 1273 K for 48 hrs in vacuum sealed quartz ampules to achieve compositional homogeneity. The ingots were cut in to suitable shapes by spark erosion technique for physical property measurements. For structural characterization the samples were pulverizedinto fine powder. The dc magnetic measurements were performed in SQUID VSM in the temperature range 5-300 K under the magnetic fields upto 5 tesla.On the other hand, *ac* susceptibility (ACS) and electrical transport measurements were performed in Physical Property Measurement System (PPMS, Model 6000) in the temperature range 2-300 K. The ACS measurements were carried out in the frequency range of 33-9333 Hz by maintaining the amplitude of the ac field at 10 Oe. Insome cases, dc fieldsin the range of 100-4000 Oe were applied. The resistivity and MR measurements were carried out using standard four-probe technique in *ac* transport (ACT, f = 133Hz) mode with source current 200 mA.

3. Results and Discussion

The powder x-ray diffraction (XRD) patterns of $Co_{55.5}TM_3Ga_{41.5}$ (TM = Co, Fe, Cr, Cu) alloys are indexed as B2 CsCl crystal structure with no significant change in lattice constant as compared to binary $Co_{58.5}Ga_{41.5}$ alloy. As shown in the Fig.1, the XRD patterns exhibit a single phase with lattice constant values2.8846 Å (TM = Co), 2.8828 Å (TM = Cr), 2.8802 Å (TM = Fe), 2.8774 Å (TM= Cu) for substituted alloys. These observations suggest that structural disorder or changes in interatomic separations are negligible.

3.1Temperature and field variation of dc magnetization

The zero field cooled (ZFC) and field cooled (FC) magnetization curves as a function of temperature are shown in Fig. 2(a). From the figure the following features can be noted: (i) as the temperature is lowered from 300 K the magnetization shows a sharp rise at certain temperature followed by a plateau. Further, at low temperature the FC, ZFC magnetization curves bifurcate and a significant reduction in ZFC magnetization value is observed. Such features indicate a double magnetic transition – a para-to-ferro magnetic (PM→FM) transition at higher temperature (indicated as T_C) and a spin glass transition at lower temperature. (ii) The Fe substituted sample shows higher T_C (~ 174 K) and magnetization values compared to those of $Co_{58.5}Ga_{41.5}$ (T_C ~ 101 K) suggesting an enhancement of ferromagnetic exchange interactions. (iii) unlike Fe substituted sample the Cr sample exhibits a broad maximum in ZFC magnetization curve resembling a single transition as observed in cluster glass or superparamagnetic systems along with bifurcation of ZFC and FC curves. From this data it is not clear whether the magnetic character observed in Cr substituted alloy is due to the

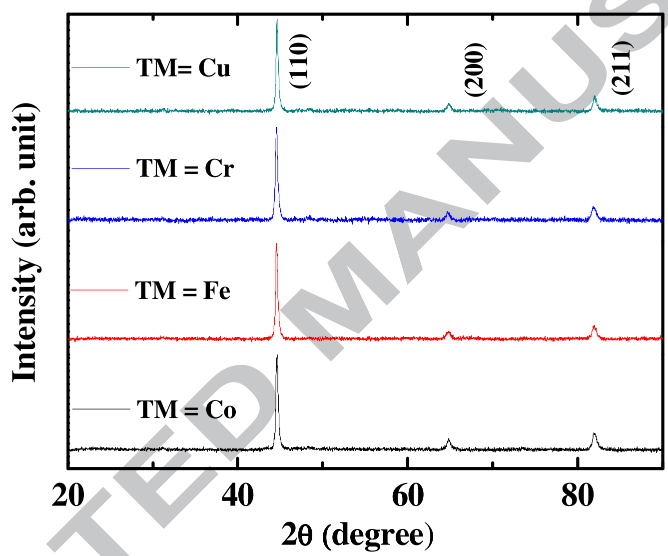

Fig. 1: Powder XRD patterns of $Co_{55.5}TM_3Ga_{41.5}$ alloys.

development of competing exchange interactions leading to a cluster glass or reentrant spin glass behavior. However, the lower values of transition temperature and saturation magnetization suggest weaker ferromagnetic exchange coupling compared to that of parent composition. The observed maximum in ZFC curve could be thought of overlapping of two magnetic transitions, which resembles a cluster glass transition. But in the present case the finite value of spontaneous magnetization at 5 K suggests the coexistence of two magnetic phases (FM and SG) at low temperature. Generally, the RSG phase appears at the FM-SG boundary of the magnetic phase diagrams. The spin configuration of low temperature RSG state consists of small spin clusters frozen in random directions on microscopic scale with [16, 17] or without [18] a trace of long-range FM order along the direction of the applied magnetic field.

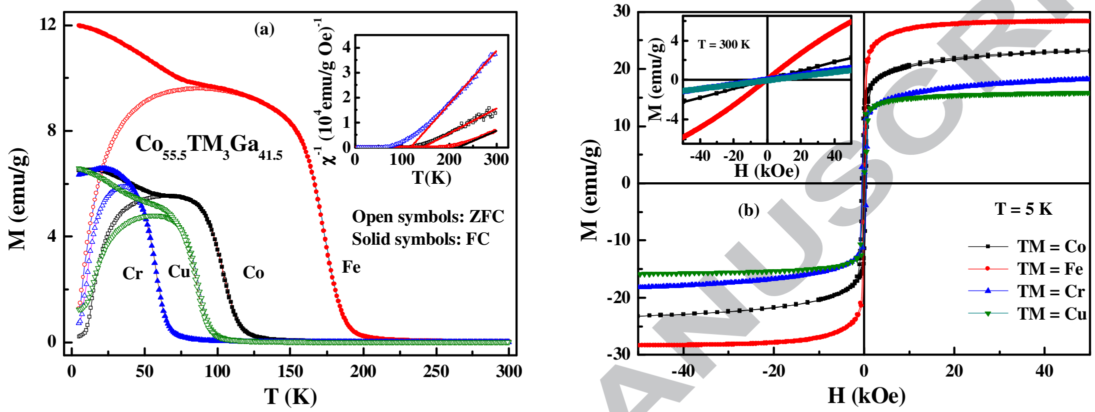

Fig. 2: (a) Magnetization as a function of temperature in ZFC and FC processes with 100 Oe field for $Co_{55.5}TM_3Ga_{41.5}$ (TM = Co, Fe, Cr, Cu), Inset: Inverse susceptibility as a function of temperature and fit to Curie-Weiss law. (b) Isothermal magnetization curves at 5 K. Inset: Isothermal magnetization curves at 300 K.

The exact nature of RSG transition is controversial and several competing models have been proposed to explain the nature of magnetization in FM phase ($T_f < T < T_C$). In general, the RSG state is expected under three distinct circumstances: (i) it is a mixed phase in which ferromagnetic order exists along the z direction with the coexistence of spin-glass order in the xy plane, (ii) consists of spin clusters of antiferromagnetic spin and the ferromagnetic matrix in which the clusters are frozen in random orientations (iii) an infinite 3D ferromagnetic matrix and the finite spin clusters (composed of a set of ferromagnetically coupled spins), which are frozen in random directions and embedded in the FM matrix. Therefore, the nature of magnetic transition in these alloys is a subject of investigation. Inset of Fig. 2(a) shows the temperature dependence of susceptibility data that fits to Curie-Weiss law far above T_C, while a pronounced departure from this is observed close to T_C indicating the existence of short-range ferromagnetic order. Further, the isothermal magnetization (*M-H*) curves at 5 K show a saturation tendency for Fe substituted alloy and finite high field susceptibility for Cr and Cu substituted alloys. These observations also suggest that the exchange coupling strength of TM elements are in the order of Co-Fe>Co-Co>Co-Cu>Co-Cr. It appears that Co-Cr and Co-Cu interactions invoke antiferromagnetic exchange and reduce the net magnetization of the alloy. A comparison between the binary and TM element substituted Co-Ga alloys suggest site disorder brings in different nature of hybridization between the TM-Ga elements. For example, $Co_{55.5}TM_3Ga_{41.5}$ (TM = Co, Fe, Cr, Cu) exhibit a double transition, while $Co_{55.5}Ga_{44.5}$ and $Co_{57}Ga_{43}$ alloys show single transition (spin-glass like) behavior [9]. Therefore, nearest *d-d* interactions as well as the site-disorder play a significant role in altering the magnetic properties. This is reflected in Arrott plots (M^2 *vs.* H/M) at 5 K (not shown in figure), which clearly demonstrated the presence of spontaneous magnetization (M_s) for all alloys of present study. A comparison of results obtained on binary and ternary systems suggest that *sp-d* hybridization also plays a role in modifying the magnetic properties. This is in agreement with band structure calculations on similar alloys [11]. The low field *M-H* curves at 5 K (Fig. 2(b)) show hysteresis with a maximum of H_c ~ 560 Oe and lower M_s value for Cr substituted alloy, suggesting development of magnetic anisotropy due to Co-Cr interactions. As expected the $M(H)$ curves at 300 K exhibit paramagnetic state in the case of all compositions. The study of spin dynamics at low temperatures by analyzing the *ac* susceptibility one can obtain more information on the nature of transition temperatures.

3.2 Temperature and frequency dependence of *ac* susceptibility

In order to ascertain the magnetic ground state of these alloys, temperature and frequency dependence *ac* susceptibility (ACS) measurements were carried out. Real, $\chi'(T)$, and imaginary, $\chi''(T)$, components of ACS were measured at different frequencies for Fe and Cr substituted alloys are shown in Fig. 3. For, Fe substituted alloy sequential magnetic phase transitions PM→FM→SG are observed on lowering the temperatures. On the other hand, for Cr substituted alloy, we observe a sharp rise in $\chi'(T)$ on lowering the temperature below ~70 K, followed by a peak around 53 K. The $\chi'(T)$ curve apparently shows single magnetic transition similar to that observed in cluster glass. However, finite value of spontaneous magnetization at 5 K indicates presence of ferromagnetic order. One can determine T_C from the inflection point in $d\chi'(T)/dT$. However, by adopting the Kouvel-Fisher (KF) method one can estimate T_C as well as critical exponent (γ), which provides useful information regarding the nature of phase transition. The advantage is that T_C and γ can be determined simultaneously without any prior knowledge of T_C [19]. The variation of zero/low field susceptibility just above T_C can be expressed using a power law: $\chi_0 \propto \left(\frac{\mathrm{T}-\mathrm{T_C}}{\mathrm{T_C}}\right)^{-\gamma}$. Alternatively, KF model can be rewritten as in Eq. (1) and linear fits to this equation

$$Y = \left\{\frac{d}{dT}\left[\ln\left({\chi_0}^{-1}\right)\right]\right\}^{-1} = \frac{\mathrm{T}-\mathrm{T_C}}{\gamma} \qquad (1)$$

yields T_C and γ values 175.9 K (56.8 K) and 1.27 (1.63), respectively, for Fe (Cr) substituted alloy. The corresponding KF plots are shown in the figure. The values of γ did not change significantly in the measured frequency range. The γ for Fe substituted alloy is close to that predicted from 3D- Heisenberg model (γ = 1.38), while γ, for Cr substituted alloy differs. However, such higher γ values have been reported for ferromagnets and RSG systems.

Now we turn our attention to discuss the low temperature transition i.e., FM→SG transition associated with a freezing temperature (T_f). The error in determination of T_f

depends on the sharpness of the peak observed in $\chi'(T)$. In cases, where distinct shoulder or anomaly appears in $\chi'(T)$ around T_f [20] the T_f is determined by extrapolating the $\chi'(T)$ data points that lie on either side of the shoulder and the intersection point of these two lines is taken as T_f.. Such distinct features are absent in the present $\chi'(T)$ data for Fe substituted alloy but, the imaginary component $\chi''(T)$ of ACS carries experimental signatures of both transitions: a weak peak around temperature T_C and a pronounced frequency dependent peaks around T_f.. On the other hand, $\chi'(T)$ for Cr substituted alloy shows a weak frequency dependence just below T_C. However, a pronounced frequency dependent maxima are observed in the $\chi''(T)$, at comparatively lower temperature. Therefore, it seems pertinent to assign the frequency dependent peak in $\chi''(T)$ as the freezing temperature $T_f(\omega)[\equiv T_p(\omega)]$, similar to that of RSG systems [21]. The T_f shifts to higher temperature with increasing ω (Fig. 3), characteristic of the non-ergodic behavior normally associated with spin glasses [22]. In general, for SG transition, $T_f(\omega)$ is defined as the temperature where the maximum relaxation time, $t \approx 1/\omega$, of the system corresponds to the measurement frequency. The divergence of the maximum relaxation time, at the spin glass transition temperature, can thereafter be investigated using dynamic scaling. On the other hand, we can also associate the maximum in $\chi''(T)$ to the slowing down due to spin glass dynamics and analyze the data using dynamic scaling models. Defining the temperature of the maximum in $\chi''(T)$ as the freezing temperature, T_f, at a specific observation time ($t \approx 1/\omega$), attempt has been made to investigate whether or not the 'critical slowing' down (CSD) model accounts for $T_f(\omega)$. According to CSD model [22]

$$\omega = \omega_0[(T^*(\omega) - T_g)/T_g]^{z\nu} \qquad (2)$$

where, ω_0 is attempt frequency, $T^*(\omega) \equiv T_p(\omega) \equiv T_f(\omega)$ is the frequency-dependent peak temperature, T_g is the spin glass transition temperature which represents infinitely slow cooled dc (equilibrium) value of $T_f(\omega \rightarrow 0)$) where the spin-spin correlation length (ξ) diverges as $\xi \sim \varepsilon^{-\nu}$ with $\varepsilon = (T-T_g)/T_g$. The critical exponent ν characterizes the divergence in ξ and z is the dynamic critical exponent, which describes the evolution of the relaxation time ($\tau \sim \xi^z$). The linear plot of $log_{10}(\omega/\omega_0)$ against $log_{10}[(T_p(\omega)- T_g)/ T_g]$ (inset of Fig. 3) is obtained by varying T_g, which demonstrates the validity of Eq. (2). The best fit to the data yields ω_0 = 5.8×10^6 (3.26×10^7) Hz, and $z\nu$ = 2.44 (5.36) (from the intercept and slope) when $T_p(\omega)$ is identified as $T^*(\omega)$ and the choice of parameter T_g = 78.1 (34.7) K is made for Fe (Cr) substituted alloy. The obtained relaxation time $\tau_0 \approx 1.7\times10^{-7}$ (3.0×10^{-8}) s for Fe (Cr) substituted alloy is higher than that reported for spin glasses ($\tau_0 \sim 10^{-11}$-10^{-12} s) with minimal spin cluster formation implying that the RSG phase is constituted by randomly magnetized spin clusters [23], instead of atomic (spin) level randomness. On the other hand, $z\nu$ falls in the range $2 \leq z\nu \leq 14$, empirically found for glassy systems. Such kind of higher τ_0 values have been observed in RSG systems. Regardless of these observations, the reasons behind such larger flipping times are still unclear and are under investigations. It is to be noted that in general, determination of T_f for RSG is less accurate compared to SG [24].

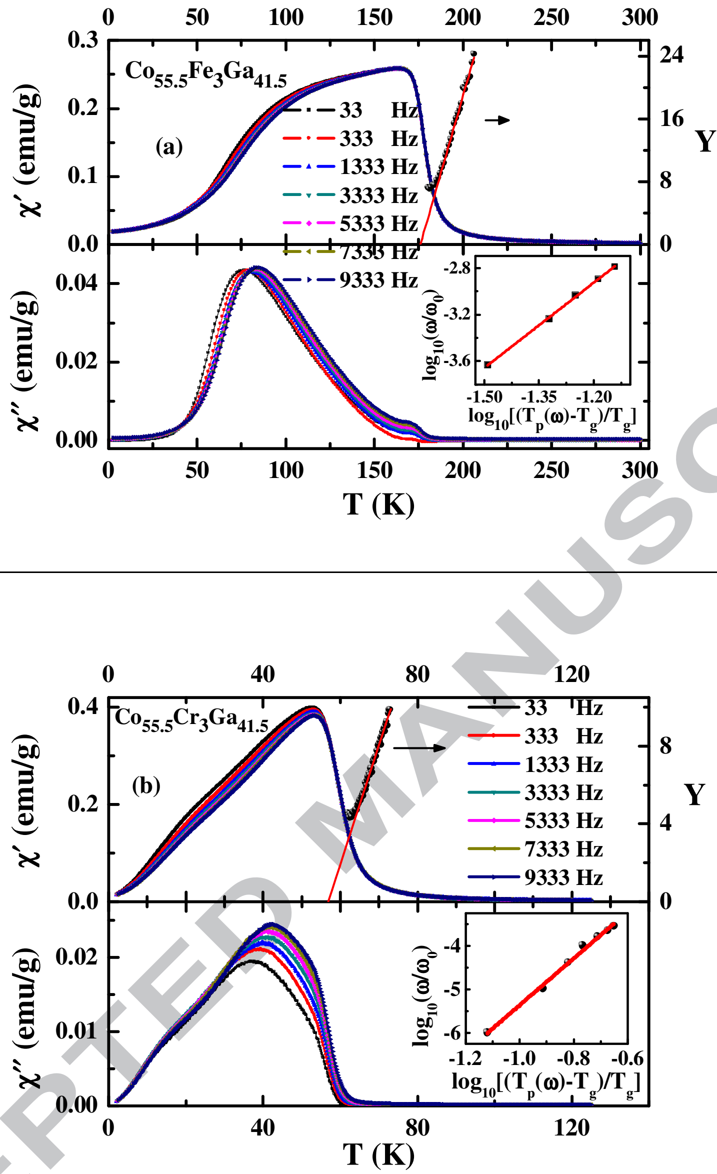

Fig. 3: Temperature variation of real component (upper panel) and imaginary component (lower panel) of ACS at different frequencies (33-9333 Hz) for Fe and Cr substituted alloys. Upper panel also shows KF plot at 33 Hz; Inset: Plot of $log_{10}(\omega/\omega_0)$ against $log_{10}[T_p(\omega) - T_g)/T_g]$ with obtained parameters T_g and ω_0 along with linear fit.

On the other hand, the CSD model fits to frequency dependence of T_f obtained from real component of ACS data for Fe substituted alloy resulted in $\tau_0 \approx 5.5\times10^{-10}$ s, and $z\nu = 5.7$ with $T_g = 78.0$ K. The exponent $z\nu$ falls in the range $2 \leq z\nu \leq 14$, while τ_0 turns out to be smaller than that obtained from the analysis of $\chi''(T)$ data, but still larger when compared to that for conventional SG. Similar order of τ_0 has been reported in RSG system [20]. On the other hand, weak frequency dependent $\chi'(T)$ data for Cr substituted alloy, yielded $\omega_0 = 6.91\times10^{12}$ Hz, and $z\nu = 4.98$ with proper choice of T_g. The value of $\tau_0 = 1.4\times10^{-13}$ s falls in the range of conventional SG, and $\varphi\left(=\frac{\Delta T_f}{T_f \Delta(\log\omega)}\right) = 0.004$ turns out to be even smaller than that of conventional SG ($\varphi \approx 0.005$ for $Cu_{1-x}Mn_x$) [22]. Thus, the real component of ACS data yields unphysical values of τ_0 and φ.

As shown in Fig 4, similar features are observed for parent alloy composition $Co_{58.5}Ga_{41.5}$. The T_C, and γ, obtained from KF plot are found to be 101.6 K, and 1.45, respectively. Further, the imaginary component exhibits double transitions with an anomaly around T_C followed by a pronounced frequency dependent peak. However, the imaginary component shows contrasting features as compared to that of Fe and Cr substituted alloys.

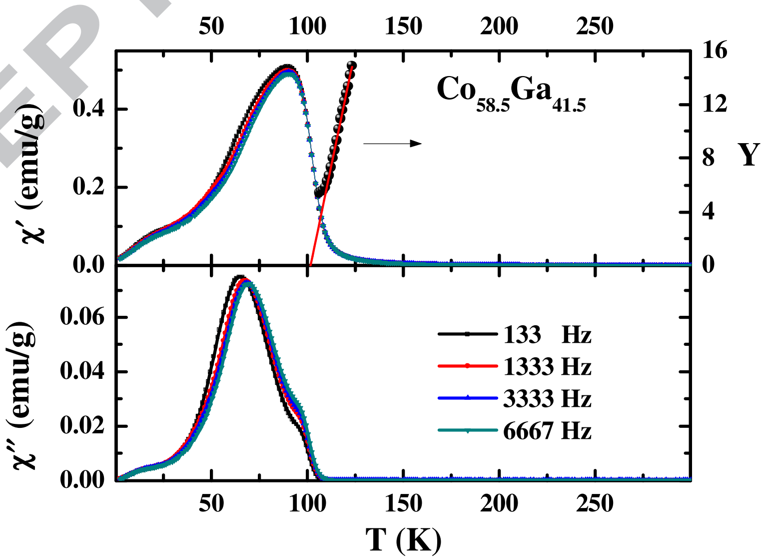

Fig. 4: Temperature variation of real component (upper panel) and imaginary component (lower panel) of ACS at different frequencies (133-6667 Hz) for parent alloy. Upper panel also shows KF plot at 133 Hz.

The peak in $\chi''(T)$ shifts to higher temperature, while the magnitude of the peak decreases with the increase in frequency. Although this is not a signature of conventional spin glasses, similar trend was observed in some glassy systems including RSG [25].

3.3 *ac* susceptibility under dc bias field

In our earlier discussion we have identified the T_C and T_f through temperature dependence of dc magnetization data as well as by analyzing $\chi'(T)$ and $\chi''(T)$ data respectively. Alternatively, *ac* susceptibility experiments under dc magnetic field help in resolving the transitions temperatures in some complex magnetic systems [26], where the T_C lies very close to T_f. In order to ascertain our earlier analysis we have carried out ACS measurements under high dc bias. Figure 5, shows dc bias effect on $\chi'(T)$, which results in development of distinct peaks near magnetic transitions with suppression of both $\chi'(T)$ and $\chi''(T)$ components in ferromagnetic phase. At low dc field (100 Oe), $\chi'(T)$ does not show well defined peak, rather it traces an onset of a shoulder (not shown in figure) at low temperature. These features are often observed in RSG or cluster glass systems. The T_f, shifts further to low temperature (Fig. 5) with the increase in dc field, which is another characteristic feature of spin glasses [17] and follows the relation $T_f(H_{dc}) = T_f(H_{dc}= 0)[1- CH^{3/2}_{dc}]$ (Inset of Fig. 5). But a strong departure from $H^{3/2}_{dc}$ behavior is observed above H_{dc}= 2000 Oe. The $H^{3/2}_{dc}$ behavior is normally associated with the Almeida-Thouless (AT) phase transition line in the Ising spin glass. Since uniaxial anisotropy is not expected the possibility of attributing of $T_f(H_{dc})$ to the AT irreversibility line can be ruled out. The other possibility is Heisenberg chiral spin glass [27] which on account of the coupling between chiral and spin degrees of freedom induced by a weak random anisotropy, predicts the $H^{3/2}_{dc}$ power law variation of T_f.

The high temperature $\chi'(T)$ peak is present even in the absence of external field, which is very close to, but below T_C, as estimated through KF method. From Fig. 5, it is observed that these peaks shift to higher temperature with the application of external dc field. Such contrast behavior in T_f and T_C, implies that the increasing field gradually destroys the frozen SG configuration and strengthen FM ordering.

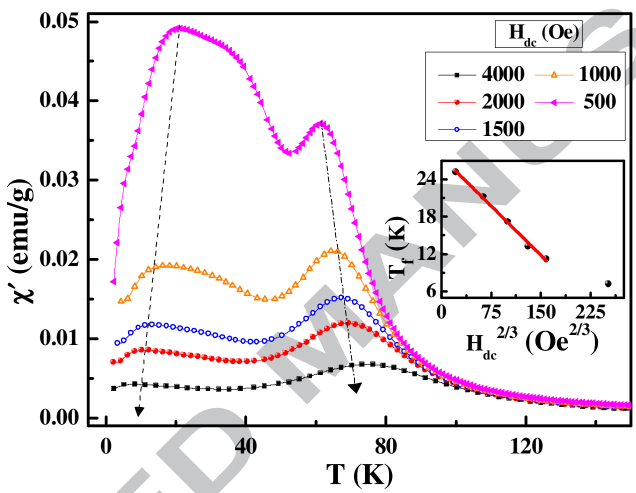

Fig. 5: Temperature variation of real component ($\chi'(T)$) of ACS under different superposed dc field, measured at a fixed frequency (133 Hz) for Cr substituted alloy. The lines are guide to the eye, where the arrows indicate the field-induced peak-shifts; Inset demonstrates the $H^{3/2}_{dc}$ power law variation of T_f.

3.4 Memory, ageing and relaxation in $Co_{55.5}Cr_3Ga_{41.5}$ alloy

In order to confirm the magnetic ground state, memory effect of Cr substituted alloy has been investigated (Fig. 6(a)) in FC protocol as proposed by Sun *et al.* [28]. The sample is cooled from high temperature (300 K) with intermittent stop at temperature T_s (around 15 K $<T_g$) in the presence of 100 Oe magnetic field. On reaching T_s, the field was switched off and aged at

T_s for ~ 7200 s. During this time the FC magnetization decreases due to relaxation. Subsequently the sample was cooled down to lowest temperature (5 K) by applying same field. This protocol leads to step-like feature of M_{FC} ($T \downarrow$) curve as shown in figure. After reaching lowest temperature, the system is warmed up with the same rate and M_{FC} ($T \uparrow$) is recorded in the presence of same applied field. The $M_{FC}(T \uparrow)$ curve obtained during warm up also exhibits a step-like shape (broad peak near T_s) and it recovers to the value of $M_{\mathrm{FC}}(T)$ around 45 K. Thus we observe memory effect for RSG in FC mode. Subsequently we have attempted to study the memory effect in ZFC protocol. However, in the limited wait time (7200 s) discernible change was not observed.

It is well established that slow decay of remanent magnetization occur in conventional spin glasses, cluster glasses, and even in RSG systems. In order to demonstrate the magnetic relaxation, the sample is cooled through T_g from high temperature (300 K) with a fixed cooling rate 3K/min in the presence of field (~ 500 Oe). At lowest temperature the field was switched-off, and the decay of magnetization was recorded as a function of time (up to 8500 s) and shown in Fig. 6(b). The remanent magnetization decays slowly and remains nonzero even after 8500 s. Further, it is observed that the stretched exponential function (Eq. 3) [22] describes the $M(t)$ behavior satisfactorily

$$M(t) = M_0 + M_g \exp\left[-\left(\frac{t}{\tau_{dc}}\right)^{\beta}\right] \qquad (3)$$

where, M_0 and M_g are related to ferromagnetic and glassy components. The values of M_g, time constant τ_{dc} and the exponent β ($0 < \beta < 1$) depend on temperature. The fits to $M(t)$ data without M_0 in Eq. 3 yields unphysical τ_{dc} and significantly smaller β values as compared to those observed in glassy systems. For classical SG systems, M_0 is treated as 0 in Eq. (3). However, a non-zero value of M_0 has been used due to the coexistence of FM and SG components [29]. With M_0, the fitted parameters are found to be M_g/M_0 = 0.28, τ_{dc} = 3385 s, and β = 0.21 for $t \geq 20$ s. Significant departures of the fitted curve from the actual data is observed at short time (t < ≈ 20 s) (Fig. 6(b)), as commonly observed in spin glasses. The non-zero values of M_0 and β indicate the signature of coexistence of FM and SG components in the relaxation process. If the changes observed in magnetic behavior are due to hybridization effects/DOS related, one can observed anomalies in electrical transport behavior in the vicinity of magnetic transitions. Hence, low temperature electrical transport studies will be useful to see the correlated nature.

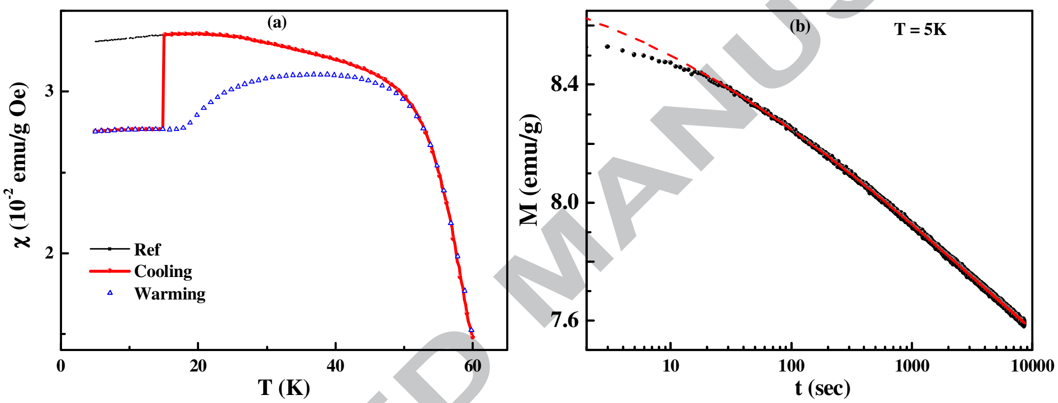

Fig. 6: (a) Memory effect measured in FC protocol for Cr substituted alloy. The solid lines are guide to the eye. (b) Remanent magnetization at 5 K (which was cooled in FC mode under 500 Oe field) plotted as a function of time. The dashed line represents the fits to the data to Eq. (3).

4. Electrical transport

4.1 Temperature dependence of resistivity:

In binary Co-Ga system electrical conductivity and magnetization at 5 K is observed to increase with Co content. This suggests either change in the density of states at Fermi level or development of spin fluctuations. Magnetic measurements on these alloys also indicated the presence of spin fluctuations in compositions close to the percolation threshold. It is well known that the spin fluctuations contribute to the transport phenomena since they scatter conduction electrons through the exchange interactions. These features understood on the basis of a two-band model, where electrons in the conduction band carry charge or heat while those in the narrow d-band contribute to the spin fluctuations which scatter the conduction electrons through the s-d exchange interaction. Therefore, to probe the transition metal atomic site without changing the non-magnetic component (Ga), we investigate the ternary alloy composition.

The normalized resistivity (ρ/ρ_{2K}) data as a function of temperature for $Co_{55.5}TM_3Ga_{41.5}$ (TM = Co, Cr, Cu, Fe) alloy is plotted in Fig.7. Low temperature data is also plotted as function of T^2, which shows a spin fluctuation contribution to Co and Cr substituted alloys. While, for Fe and Cu substituted samples, this contribution becomes weaker probably due to stronger exchange (spin wave contribution). In the case of Cr substitution, temperature dependence of resistivity, $\rho(T)$, data shows negative TCR at low temperature and changes sign with temperature exhibiting a minimum in the resistivity curve at a certain temperature ($T_{\min}$). The resistivity increases monotonically up to a temperature with a gradual change in the slope and at higher temperatures, a saturation tendency is observed. On the other hand, for Cu, Co and Fe additions, the low temperature minimum disappears and positive TCR has been observed in the complete temperature range of present study. This observation is in agreement with field and composition dependence of binary alloys. It is interesting to point out here that a change in slope of $\rho(T)$ curve is observed above their respective T_C. The temperature at which slope change in $\rho(T)$ (near T_C) is observed is denoted as T_i and given in Table 1. The low temperature anomaly and the higher residual resistivity value in Cr substituted alloy could be due to antiferromagnetic coupling as evident from magnetic study. On the other hand, for Fe substituted alloy the nature of $\rho(T)$ curve resembles higher Co content Co–Ga alloy, which is a direct consequence of strong enhancement of the ferromagnetic character in this alloy.

4.2 Temperature and field dependence of Magnetoresistance:

The field dependence of $\rho(T)$ data showed that the residual resistivities in Co and Cr substituted alloys are greatly suppressed by the application of field. However, significant field effect was also noticed around their T_C and progressively decreases at higher temperatures. The field effects on $\rho(T)$ for Cu and Fe substituted alloys are more pronounced around T_C rather than at low temperature. In order to investigate the correlation between magnetic and transport behavior, the temperature variation of magnetoresistance, MR(T), and magnetization $M(T)$ are plotted in Fig. 8. The MR(T) curves for parent and Cr substituted alloys show maximum MR (negative) at low temperature and progressively decrease with increasing temperature exhibiting an anomaly near its T_C. However, the MR value in Cr substituted alloy is significantly lower than that of parent alloy.

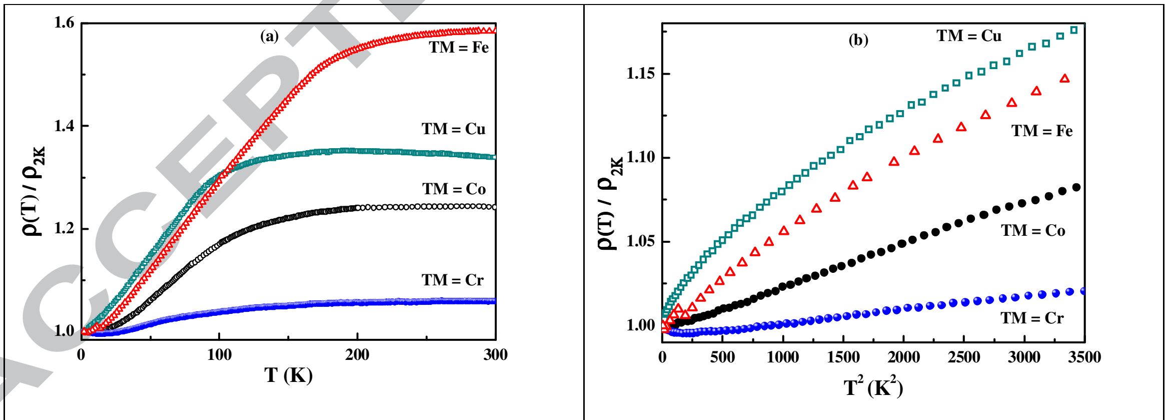

Fig. 7: Normalized resistivity as a function of (a) temperature (T) (b) T^2 of $Co_{55.5}TM_3Ga_{41.5}$ (TM = Co, Cr, Cu, Fe).

Table 1: Various parameters obtained from magnetic and electrical transport study of $Co_{55.5}TM_3Ga_{41.5}$.

$Co_{55.5}TM_3Ga_{41.5}$ TM	M_{5K}(emu/g) H = 50 kOe	ρ_{5K} ($\mu\Omega$ cm)	T_i (K)	T_C(K)
Co	23.09	219	100	103
Cr	18.20	403	61	57
Cu	15.86	237	92	86
Fe	28.33	224	173	175

The MR(T) curves for Cu and Fe substituted alloys show finite MR (negative) at low temperature and increases further with increasing temperature followed by a sharp upturn around its T_C. The maximum MR at T_C suggests that the critical spin fluctuations contributing to ρ are greatly suppressed by external magnetic field. At temperatures higher than T_C, the MR value decreases significantly as seen from the figure.

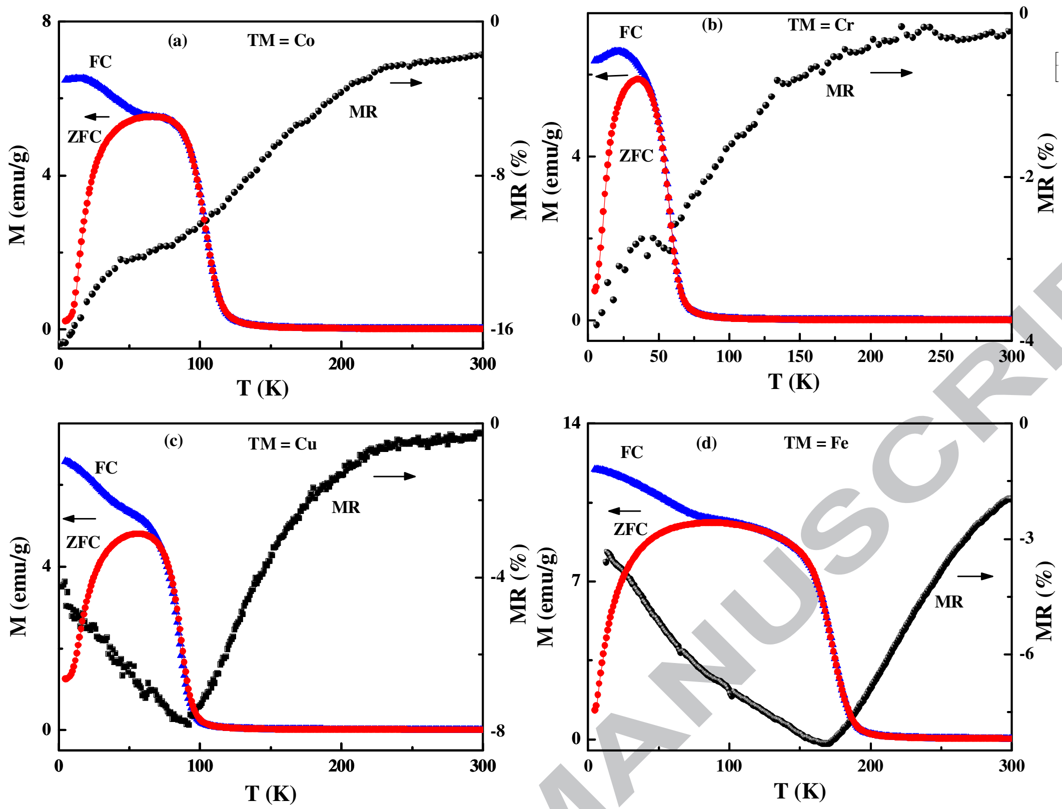

Fig. 8: Magnetization and MR as a function of temperature for $Co_{55.5}TM_3Ga_{41.5}$ (TM = Co, Cr, Cu, Fe). MR was measured at 80 kOe (90 kOe) for substituted (parent) alloys.

Further, as shown in Fig. 9, the field variation of MR measurements were carried out at selected temperatures based on magnetic and MR(T) characteristics. It is interesting to see that only $Co_{58.5}Ga_{41.5}$ composition presents a maximum MR at lowest measuring temperature (Fig. 9(a, b)). Substitution of transition metal element (Fe, Cr, Cu) in place of Co results in deterioration of MR properties compared to that of $Co_{58.5}Ga_{41.5}$. The MR(H) at low temperature could be well described by Khosla and Fischer model (Eq. 4) [30] rather than theoretically predicted expressions for spin-wave contributions in weak itinerant-electron ferromagnets [31]. In order to improve the quality of fit a weak-localization term ($H^{1/2}$) has been added to Eq. 4.

$$\frac{\Delta\rho}{\rho} = -B_1 \ln\left(1 + B_2^2 H^2\right) \qquad (4)$$

For cobalt substituted alloy, MR(H) data below 50 K (above which anomaly is observed as seen from MR(T) data in Fig. 8(a)) is fitted to Eq. 4 (Fig. 9(a)). The fitted parameters are given in Table 2, which show consistency with the increasing temperature. On the other hand, Cr substituted alloy although exhibits same functional form, the maximum MR is lower than that of parent alloy. On the other hand, for Fe and Cu substituted alloys the maximum MR is observed around their respective T_C's (Fig. 9(c,d)). The maximum MR (≈ -8%) is observed for Cu substituted alloy around its T_C under the application of maximum applied field (80 kOe). In order to assess the functional form of MR(H) at temperature very close to T_C a simple power law of the form MR ~ H^n was tried, rather than any explicit expression based on spin fluctuation theory. Interestingly, the fit yielded reasonably values of $n \approx 0.72$ (0.69) for Cu (Fe) substituted alloy. Such power law dependence can be understood in terms of a theory, due to Balberg [32] that takes into account the critical fluctuations of the order parameter (spontaneous magnetization) and yields the expression

$$\frac{\Delta\rho}{\rho} \sim h^{(1-\alpha)/\beta\delta} \qquad (5)$$

(where, $h = \mu_B H/kT$ and the α, β, and δ are standard critical exponents) for the variation of MR(H) around T_C for a ferromagnet.

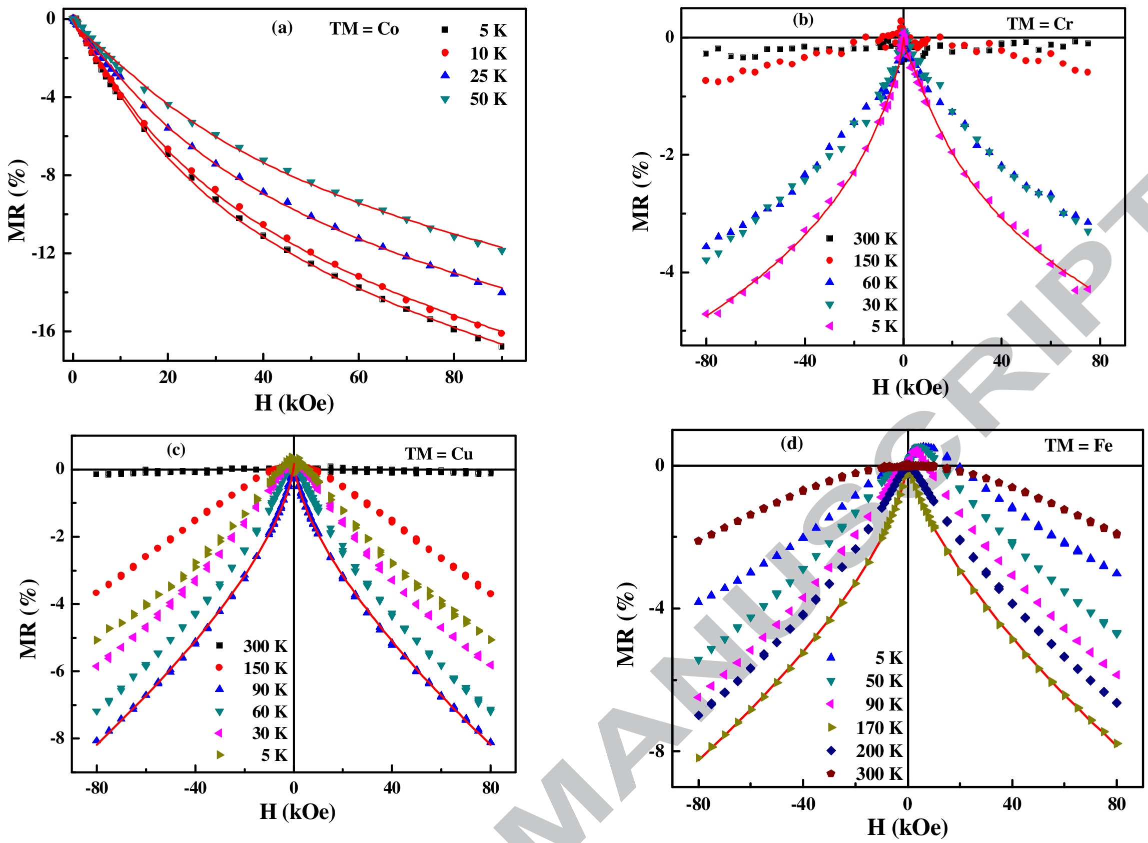

Fig. 9: MR as a function of field at different temperatures for $Co_{55.5}TM_3Ga_{41.5}$ (TM = Co, Cr, Cu, Fe). The lines are fits to the data (see text).

Table 2: Parameters obtained from the fitted data in Fig. 9(a).

T (K)	B_1	B_1^2 (10^{-8} Oe^{-2})
5	2.37	1.55
10	2.26	1.36
25	2.00	0.97
50	1.85	0.61

From the experimental observations it is seen that critical concentration of binary alloy $Co_{58.5}Ga_{41.5}$ exhibits mixed interactions (ferro & antiferro). If small amount of Co is replaced by magnetic or non-magnetic element the magnetic phase either becomes more ordered or disordered depending on the nature of TM-element. This also results in some changes low temperature electrical transport. For e.g., (i) if the exchange interactions are strengthened the spin disorder scattering decreased, resistivity minimum disappears and TCR becomes positive. The MR value decreases indicating reduction of spin disorder scattering. However, a marginal increase in MR is observed at transition temperature. (ii) Substitution of Cr magnetic disorder increases (AFM phase), which resulted in Kondo like minimum in resistivity. Application of field suppresses the minimum but low MR values are observed.

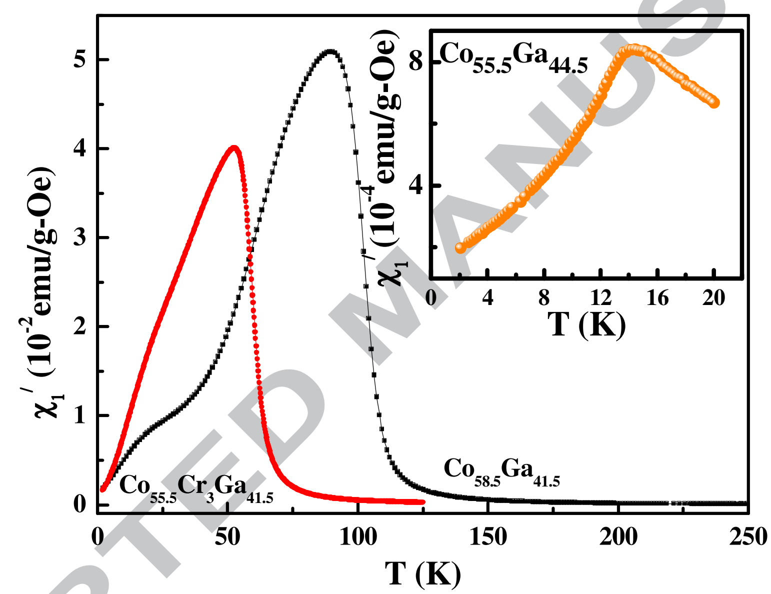

Fig.10 Temperature dependence of *ac* susceptibility of $Co_{55.5}Cr_3Ga_{41.5}$ and $Co_{58.5}Ga_{41.5}$, inset: ACS of $Co_{55.5}Ga_{44.5}$ composition.

Comparison of magnetic characteristics of three compositions, $Co_{55.5}Ga_{44.5}$, $Co_{55.5}Cr_3Ga_{41.5}$ and $Co_{58.5}Ga_{41.5}$, suggests that the Co-Ga nearest neighbor decreases moment faster than Co-Cr. A typical temperature dependence of *ac* susceptibility plot is shown in Fig.10, where the inset shows spin-glass behavior for $Co_{55.5}Ga_{44.5}$ composition. However, both $Co_{55.5}Cr_3Ga_{41.5}$

and $Co_{58.5}Ga_{41.5}$ compositions show RSG behavior. These studies indicate $Co_{58.5}Ga_{41.5}$ is a critical composition with required ingredients to obtain maximum MR.

5. Summary and Conclusion

Low temperature magnetic and electrical transport properties of transition metal (TM) substituted Co-Ga alloys at critical composition have been investigated. From the rigorous analysis of the high precision magnetic and electrical transport data the following conclusions are drawn.

(i) The $Co_{55.5}TM_3Ga_{41.5}$ (TM = Co, Cr, Fe, Cu) exhibits a double magnetic transition, which is different from $Co_{55.5}Ga_{44.5}$ composition. From dc and *ac* magnetic data reentrant spin glass transition has been proposed, ruling out the possibility of cluster glass or superparamagnetic state as claimed by earlier authors. However, transition temperatures vary significantly suggesting apart from site disorder the nature of exchange interaction Co-TM plays significant role.

(ii) The smeared magnetic transition (T_f) observed in these alloys was identified through dynamic scaling analysis of real and imaginary components of AC susceptibility. The higher relaxation time suggests that the RSG phase is constituted by randomly magnetized spin clusters. The RSG state for Cr substituted alloy exhibits memory effect in FC protocol and the relaxation could be described by the stretched exponential function.

(iii) From the magnetic field and substitution effects it has been established that the magnetic and electrical transport properties are correlated in this system. The impurity band model fits well to MR as a function of field.

(iv) From the present MR data it is shown that the MR(*T*) data is useful and alternative method to identify the reentrant spin glass transition.

Acknowledgement

Authors would like to thank the Department of Physics, IIT Madras, for some specific magnetic measurements in the SQUID-based vibrating sample magnetometer.

References

[1] P. Coleman, Heavy Fermions: Electrons at the Edge of Magnetism, *Handbook of Magnetism and Advanced Magnetic Materials*, *Volume 1: Fundamentals and Theory* (John Wiley & Sons) (2007).

[2] J. Spałek and A.Slebarski, *Journal of Physics: Conference Series* **273** (2011) 012055.

[3] M. Jourdan, J.Mina´r, J. Braun, A. Kronenberg, S. Chadov, B. Balke, A. Gloskovskii, M. Kolbe, H. J. Elmers, G. Scho¨nhense, H. Ebert, C. Felser and M. Kla¨ui, *Nat. Commun.* **5** (2014) 3974.

[4] S. Ubaid-Kassis, T. Vojta and A. Schroeder, *Phys. Rev. Lett.* **104** (2010) 066402.

[5] Ch. Venkatesh, V. Srinivas, V.V. Rao, S.K. Srivastava, P. S. Babu, J. *Alloys Compd.* **577** (2013) 417.

[6] A.K. Grover, S.K. Malik, C. Radhakrishnamurty and R. Vijayaraghavan, Solid. State Commun. 32 (1979) 1323.

[7] M. K. Chattopadhyay, S. B. Roy, S. Chaudhary, K. J. Singh and A. K. Nigam, *Phys. Rev. B* **66** (2002) 174421.

[8] C. S. Lue, Y. Oner, D. G. Naugle, and J. H. Ross, Jr., *Phys. Rev. B* **63** (2001) 184405.

[9] C.S. Lue, W.J. Lai, C.L. Huang, Y.H. Lee, *J. Magn. Magn. Mater.* 282 (2004) 334.

[10] B. A.D' Santhoshini and S.N. Kaul, *J. Magn. Magn. Mater.* **272** (2004) 493.

[11] N. Stefanou, R.Zeller and P.H. Dederichs, *Phys. Rev. B* **35** (1987) 2705.

[12] M.W. Meisel, W.S. Zhou, J.R. Owers-Bradley, Y. Ochiai, J.O. Brittain and W.P. Halperin, *J. Phys. F: Met. Phys.* **12** (1982) 317.

[13] D.M.R. Lo Cascio and H. Bakker, *Phys. Stat. Sol. (a)* **135** (1993) 611.

[14] S.M. Yasin, R. Saha, V. Srinivas, S. Kasiviswanathan and A.K. Nigam, *J. Magn. Magn. Mater.* **418** (2016) 158.

[15] R. Cywinski , J.G. Booth and B.D. Rainford, *J. Appl. Cryst.* **11** (1978) 641.

[16] M. Gabay and G.Toulouse, *Phys. Rev. Lett.* **47** (1981) 201.

[17] S. Niidera and F. Matsubara, *Phys. Rev. B* **75** (2007) 144413.

[18] S.B. Roy and M.K. Chattopadhyay, *Phys. Rev. B* **79** (2009) 052407.

[19] J.S. Kouvel and M.E. Fisher, *Phys. Rev*. **136** (1964) A1626.

[20] B.R. Kumar and S.N. Kaul, *J. Magn. Magn. Mater.* **418** (2016) 37.

[21] K. Jonason, J. Mattsson and P. Nordblad, *Phys. Rev. B* **53** (1996) 6507.

[22] J.A. Mydosh, *Spin Glasses: An Experimental Introduction* (Taylor & Francis, London) (1993).

[23] A. Haldar, K.G. Suresh and A.K. Nigam, *Euro. Phys. Lett.* **91** (2010) 67006.

[24] M. Viswanathan and P.S. Anil Kumar, *Phys. Rev. B* **80** (2009) 012410.

[25] A. Kumar, R.P. Tandon and V.P.S. Awana, *J. Appl. Phys.* **110** (2011) 043926.

[26] M. Balanda, K. Falk, K. Griesar, Z. Tomcowicz and W. Haase, *J. Magn. Magn. Mater.* **205** (1999) 14.

[27] H. Kawamura, *J. Phys. Soc. Jpn.* **79** (2010) 011007.

[28] Y. Sun, M.B. Salamon, K. Garnierand, R.S. Averback, *Phys. Rev. Lett.* **91** (2003) 167206.

[29] D. Kumar, *J. Phys.: Condens. Matter*. **26** (2014) 276001.

[30] B.P. Khosla and J.R. Fischer, *Phys. Rev. B* **2** (1970) 4084.

[31] S.N. Kaul, *J. Phys.: Condens. Matter* **17** (2005) 5595.

[32] I. Balberg, *Physica B* **91** (1977) 71.